

# Lifetime Characterization of Extreme Wave Localizations in Crossing Seas

Yuchen He<sup>1,2</sup> Jinghua Wang<sup>1,3,4†</sup>, Jingsong He<sup>5</sup>, Ye Li<sup>2</sup>, Xingya Feng<sup>2</sup>, and Amin Chabchoub<sup>6,7</sup>

<sup>1</sup>Department of Civil and Environmental Engineering, The Hong Kong Polytechnic University, Hong Kong SAR

<sup>2</sup>Department of Ocean Science and Engineering, Southern University of Science and Technology, Shenzhen 518055, China

<sup>3</sup>Research Institute for Sustainable Urban Development, The Hong Kong Polytechnic University, Hong Kong SAR

<sup>4</sup>Shenzhen Research Institute, The Hong Kong Polytechnic University, Shenzhen 518057, China

<sup>5</sup>Institute for Advanced Study, Shenzhen University, Shenzhen 518060, China

<sup>6</sup>Disaster Prevention Research Institute, Kyoto University, Uji, Kyoto 611-0011, Japan

<sup>7</sup>Department of Infrastructure Engineering, The University of Melbourne, Parkville, Victoria 3010, Australia

(Received xx; revised xx; accepted xx)

Rogue waves (RWs) can form on the ocean surface due to quasi-four wave resonant interaction or superposition principle. Both mechanisms have been acutely studied. The first of the two is known as the nonlinear focusing mechanism and leads to an increased probability of rogue waves when wave conditions are favourable, i.e., when unidirectionality and high narrowband energy of the wave field are satisfied. This work delves into the dynamics of extreme wave focusing in crossing seas, revealing a distinct type of nonlinear RWs, characterized by a decisive longevity compared to those generated by the dispersive focusing mechanism. In fact, through fully nonlinear hydrodynamic numerical simulations, we show that the interactions between two crossing unidirectional wave beams can trigger fully localized and robust development of RWs. These coherent structures, characterized by a typical spectral broadening then spreading in the form of dual bimodality and recurrent wave group focusing, not only defy the weakening expectation of quasi-four wave resonant interaction in directionally spread wave fields, but also differ from classical focusing mechanisms already mentioned. This has been determined following a rigorous lifespan-based statistical analysis of extreme wave events in our fully nonlinear simulations. Utilizing the coupled nonlinear Schrödinger framework, we also show that such intrinsic focusing dynamics can also be captured by weakly nonlinear wave evolution equations. This opens new research avenues for further explorations of these complex and intriguing wave phenomena in hydrodynamics as well as other nonlinear and dispersive multi-wave systems.

## 1. Introduction

Since the recording of the New Year or Draupner wave in 1995, fundamental research related to ocean rogue wave (RW) investigation has attracted much attention in recent decades due to its key relevance in coastal, ocean, and arctic engineering applications (Kharif *et al.* 2008; Osborne 2010; Ducrozet *et al.* 2020; Mori *et al.* 2023; Toffoli *et al.*

† Email address for correspondence: jinghua.wang@polyu.edu.hk

2024; Klahn *et al.* 2024). Assuming the wave being unidirectional, the formation of RWs can be explained as a result of wave superposition (Longuet-Higgins 1974; Fedele *et al.* 2016; McAllister *et al.* 2019; Häfner *et al.* 2021) or modulation instability (MI) (Benjamin & Feir 1967; Zakharov 1968; Tulin & Waseda 1999; Chabchoub *et al.* 2011; Bonnefoy *et al.* 2016). Both focusing mechanisms are equally important depending on the wave conditions at play (Dudley *et al.* 2019; Waseda 2020). The nonlinear mechanism in form of MI, along with its manifestation in complex sea states (Tulin 1996; Waseda *et al.* 2009; Onorato *et al.* 2010; Gramstad *et al.* 2018; Toffoli *et al.* 2024), has been extensively studied as a key mechanism for wave group focusing. However, the predominance of quasi-four wave resonant interactions for irregular ocean waves in crossing seas with strong directional spreading is considered to be less evident compared to unidirectional wave field counterparts due to the violation of critical assumptions such as unidirectionality and narrowband spectral conditions (Janssen 2003; Mori *et al.* 2011; Fedele *et al.* 2016; Tang *et al.* 2021; Häfner *et al.* 2023). On the other hand, a recent experimental observation of nonlinear focusing dynamics in standing water waves (He *et al.* 2022) has shown that MI could still lead to notable amplifications in wave heights for such states. Standing waves can be indeed considered as a simplified specific type of crossing sea state with an aperture angle of 180 degrees. These findings further illustrate the complex nature of nonlinear wave interactions in complex configurations.

Furthermore and in contrast to the dispersive focusing mechanism in directional wave fields, numerical studies have postulated an increased likelihood of RW formation in coupled two-wave systems by considering weak nonlinearity in the modelling of crossing seas, with the limitations that both wave fields have the same peak frequency and are narrowband (Grönlund *et al.* 2009; Liu *et al.* 2022). Notably, Liu *et al.* (2022) made a successful attempt to study the crossing RW shape under varying crossing angles and spectral shapes. This approach goes beyond traditional RW investigations, which mainly focus on spectral evolution, exceedance probability distributions, and kurtosis progression. The latter work also highlights that the shape of freak waves is more influenced by the crossing angle between wave components rather than the frequency or directional spectral bandwidth. The coupled nonlinear Schrödinger equation (CNLS), according to Okamura (1984); Onorato *et al.* (2006), and its higher-order forms (Gramstad & Trulsen 2011; Gramstad *et al.* 2018) are a commonly used frameworks for describing the dynamics of wave envelope interactions in crossing seas (Cavaleri *et al.* 2012). Indeed, the directional (2D+1) NLS and CNLS frameworks have become essential in understanding the fundamental wave hydrodynamics together with the emergence of localized and directional wave patterns, such as RWs (Chabchoub *et al.* 2019; Steer *et al.* 2019; He *et al.* 2022). However, it still remains unknown whether the weakly nonlinear wave evolution equations can sufficiently predict the occurrence of all possible RWs, which can occur also in crossing seas. For example, theoretical studies such as in (Guo *et al.* 2020) based on the Davey-Stewartson (DS) equation (Davey & Stewartson 1974) underline that directional perturbation can trigger strong localizations in time and directional space. Fully nonlinear numerical simulations also predict the spanwise wave instability with some success (Fructus *et al.* 2005b). These extreme events cannot obviously be predicted by the classical unidirectional NLS framework with their famed breather solutions (Akhmediev *et al.* 1985; Peregrine 1983; Chabchoub *et al.* 2011; Tikan *et al.* 2022). On the other hand, the directional NLS can be modified to accommodate exact solutions of the unidirectional and integrable NLS (Saffman & Yuen 1978; Chabchoub *et al.* 2019; Waseda *et al.* 2021) and can describe the dynamics of modulationally unstable short-crested waves.

To address the remaining key questions as discussed above, our numerical study, which

is based on the fully nonlinear numerical framework developed by Wang *et al.* (2021a), reveals the existence of a novel type of nonlinear and fully localized RWs, i.e., extreme localized waves in directional space and time, which are distinct in their lifetime from the cases generated as a result of wave overlap. The procedure is initiated by accounting for the wave potential's slow variation due to wave nonlinearity in the crossing sea state during the wave data analysis while the crossing New Wave Theory (Taylor & Williams 2004) is adopted as the interference model dynamics for two generated JONSWAP sea states. In this context, we introduce a lifetime parameter we refer to as lifespan  $t_{LS}$  of a RW event encompassing several consecutive RWs, which was adopted for similar purpose in previous works (Chabchoub *et al.* 2012; Kokorina & Slunyaev 2019) and as will be further elaborated upon in detail in the manuscript. Based on the above, we reveal that fully localized RW elevations and their characteristic directional pattern are strongly correlated with their lifespans  $t_{LS}$ . The longer  $t_{LS}$  of an extreme wave event, the more it differs from a large-amplitude wave created by the interference principle (Taylor & Williams 2004; Mathis *et al.* 2015; Birkholz *et al.* 2016; Fedele *et al.* 2016). In the same time, the wave energy exhibits a dual bimodal frequency evolution trend (Osborne & Ponce de León 2017; Toffoli *et al.* 2010) in the spreading directional spectrum. Differently than (Liu *et al.* 2022), we do not consider several crossing angles, but rather focus on one particular angle and vary the peakedness parameter of the JONSWAP wave field realizations, i.e. the energy distribution of each of the colliding wave field, and classify the RW events based on their longevity. Finally, we identify a new type of fully localized RW structures characterized by its unique long lifespan  $t_{LS}$  and *full-spatial localization*, i.e., in the mean wave direction, transverse direction, time, and considering the emergence of wave focusing recurrence. Despite having similar features to breathers, such dynamics cannot be predicted by the classical NLS or MI formalism that are applicable only for unidirectional waves.

## 2. Numerical Methods

Our study embraces a fully and a weakly nonlinear numerical scheme, which will be described in detail below, together with details on the cross wave field initialization.

### 2.1. The Enhanced Spectral Boundary Integral Wave Model: Configuration, Verification, and Validation

The Cartesian coordinate system is adopted here with  $\mathbf{x} = (x, y)$  being horizontal and  $z$  being vertical coordinates. The still deep-water level is at  $z = 0$ . Unless otherwise specified, the variables are being non-dimensionalized, i.e., the distance ( $\mathbf{x}$ ,  $z$ , and time  $t$ ) are multiplied by the peak wavenumber  $k_p$  and angular frequency  $\omega_p = \sqrt{gk_p}$ , respectively.

The potential flow theory assumes that the fluid is inviscid and irrotational, leading to velocities written as gradients of velocity potential  $\phi$ , rescaled by  $\sqrt{k_p^3/g}$ . The primary advantage of using the velocity potential is that it is a scalar quantity. Therefore, the number of unknowns is reduced compared to the Euler or Navier-Stokes equations, as the velocity vectors can be obtained directly by calculating the gradient of the velocity potential.

The free surface boundary conditions for the potential flow wave theory consists of those on the water free surface  $z = \eta(\mathbf{x}, t)$ :

$$\frac{\partial \eta}{\partial t} + \nabla \phi \cdot \nabla \eta - \frac{\partial \phi}{\partial z} = 0, \quad (2.1)$$

$$\frac{\partial \phi}{\partial t} + \frac{1}{2} \left[ |\nabla \phi|^2 + \left( \frac{\partial \phi}{\partial z} \right)^2 \right] + \eta = 0, \quad (2.2)$$

where  $\nabla = (\partial_x, \partial_y)$  is the horizontal gradient operator.

Eqs.(2.1) and (2.2) are identical to the canonical pair derivable from the Hamiltonian water wave system (Zakharov 1968). They can be rewritten as a skew-symmetrical form (Fructus *et al.* 2005a):

$$\frac{\partial \Psi}{\partial t} + \mathcal{A}\Psi = \mathcal{N}, \quad (2.3)$$

where:

$$\Psi = \begin{pmatrix} k\mathcal{F}\{\eta\} \\ k\omega\mathcal{F}\{\tilde{\phi}\} \end{pmatrix}, \quad \mathcal{A} = \begin{bmatrix} 0 & -\omega \\ \omega & 0 \end{bmatrix}, \quad \mathcal{N} = \begin{pmatrix} k \left( \mathcal{F}\{V\} - k \tanh(kh)\mathcal{F}\{\tilde{\phi}\} \right) \\ \frac{k\omega}{2}\mathcal{F}\left\{ \frac{(V + \nabla\eta \cdot \nabla\tilde{\phi})^2}{1 + |\nabla\eta|^2} - |\nabla\tilde{\phi}|^2 \right\} \end{pmatrix} \quad (2.4)$$

and  $\tilde{\phi} = \phi(\mathbf{x}, z = \eta, t)$  denotes the velocity potential on free surface,  $V = \sqrt{1 + |\nabla\eta|^2} \partial\phi/\partial n$  is the vertical velocity of the surface elevation, while  $\mathcal{F}\{\psi\}$  is the Fourier transform defined as:

$$\mathcal{F}\{\psi\} = \iint_{-\infty}^{\infty} \psi e^{-i\mathbf{k} \cdot \mathbf{x}} d\mathbf{x}, \quad (2.5)$$

with  $\mathcal{F}^{-1}\{\psi\}$  being its inverse transform and  $i = \sqrt{-1}$ . The Fourier transform is implemented numerically by using the Fast Fourier Transform (FFT).

Equation (2.3) can be further reformulated as:

$$\Psi(t) = e^{-\mathcal{A}(t-t_0)} \left[ \Psi(t_0) + \int_{t_0}^t e^{\mathcal{A}(t-t_0)} \mathcal{N} dt \right], \quad (2.6)$$

and can be used as the prognostic equation for updating unknowns  $\eta$  and  $\tilde{\phi}$  in time with the integration term evaluated by using a six-stage fifth-order Runge-Kutta method with embedded fourth-order solution (Clamond *et al.* 2007; Wang & Ma 2015). In general, to keep the difference below 1%, the time step size is automatically adjusted to about 1/20 peak wave period. For large spatio-temporal simulations of strongly nonlinear waves, a tolerance of 0.1% is selected corresponding to a time step size of about 1/50 peak wave period, which applies to the crossing sea simulations in the present study.

In order to update the solutions  $(\eta, \tilde{\phi})$ , the velocity  $V$  needs to be diagnosed by solving the boundary integral equation of Green's theorem. A successive approximation approach can be adopted, and the total vertical velocity is expressed as  $V = \sum V_m$ , where  $m$  represents the order of the nonlinearity  $\mathcal{O}(\varepsilon^m)$ , where the expansion parameter  $\varepsilon$  denotes the wave steepness. For simplicity, the recurrence formula for estimating  $V_m$  in the fully nonlinear Enhanced Spectral Boundary Integral (ESBI) wave model in deep-water starts with:

$$\mathcal{F}\{V_m\} = k\mathcal{F}\{\tilde{\phi}\}, \quad (2.7)$$

and then the remaining velocities in Fourier domain will be calculated by:

$$\mathcal{F}\{V_m\} = \sum_{j=1}^{m-1} -\frac{k^j}{j!} \mathcal{F}\{\eta^j V_{m-j}\} - \frac{k^{m-2}}{(m-1)!} i\mathbf{k} \cdot \mathcal{F}\{\eta^{m-1} \nabla\tilde{\phi}\}, \quad (2.8)$$

for  $m \geq 2$ .

In this pseudo-spectrum method, the  $2/(m+1)$ -rule is used here for anti-aliasing treatment, which is equivalent to the zero-padding method (Canuto *et al.* 1987). We emphasize that a smoothing technique is not required here, and the present model is very stable for the cases without appearance of breaking waves. The model has been comprehensively verified and validated for simulating a variety of highly-nonlinear wave phenomenon, crossing seas, and laboratory experiments (Wang *et al.* 2018, 2021a; Wang 2023).

Before initiating our study, we recall the commonly used definition of a RW, namely having a crest height  $\eta_c$ , exceeding at least 1.25 times the significant wave height  $H_s$ , i.e.,  $\eta_c > 1.25H_s$ . In a Gaussian sea state  $H_s$  is approximated of being four times the standard deviation of the entire water surface elevation. This threshold is based on previous studies and represents a significant deviation from the mean wave height (Kharif *et al.* 2008; Gramstad *et al.* 2018; Mori *et al.* 2023). In this context, we define  $t_{LS}$  as the duration or the lifetime of a series of observed sequence of extreme waves belonging to the same RW event. This will be clarified and discussed later on in the manuscript.

The numerical setup is described as next. The computational domain of the simulations covers  $40 \times 40$  peak wavelengths, and is resolved into  $1024 \times 512$  collocation points in  $x$  (along-wave) and  $y$  (cross-wave) directions, respectively. While the selected domain size and resolution in space ensure that the Fourier modes up to seven and three times peak wavenumber in the  $x$ - and  $y$ - directions, respectively, are aliasing-free. The reference sea state and wave surface condition is based on the JONSWAP spectrum (Hasselmann *et al.* 1973) with different peakedness factors  $\gamma = 1, 2, 3, 4, 6, \text{ and } 9$  with crossing wave field of steepness  $k_p H_s = 0.28$ . These two wave systems with same peak frequency  $f_p$ , peakedness parameter  $\gamma$ , significant wave height  $H_s$ , and random phases cross-interact at an aperture angle of 40 degrees, which corresponds to the most hazardous angle leading to the highest probability distribution tail (Toffoli *et al.* 2011; Cavaleri *et al.* 2012; Bitner-Gregersen & Toffoli 2014). Several wave probes are deployed every four peak wavelengths along the center of the domain in  $x$ -direction. The wave generation zone is deployed along  $x = 0$  and absorbed at a distance near the other end. Each simulation lasts for 1000 peak periods  $T_p$  (equivalent to a typical three hours sea state), and four realizations are performed.

A snapshot of the simulated cross free surface as described above is shown in Figure 1. Several large amplitude wave groups can be observed in directional space at a particular instant of time. We would like to emphasize that wave breaking is inevitable under such wave conditions. To stabilize the simulations, the low-pass filter is employed to suppress the breaking (Xiao *et al.* 2013). This filter is shown to well represent the energy dissipation quantitatively over a broad range of wave steepness, breaker types and directional spreading. We refer to (Wang *et al.* 2021b) for a direct comparison of the model simulations with laboratory experiments, involving the evolution of kurtosis and wave crest exceedance probability trends.

## 2.2. The Hydrodynamic Coupled Nonlinear Schrödinger Equation

The purpose for introducing the CNLS is two-fold. It is adopted to compare the strong RW localizations, as obtained from the fully nonlinear ESBI simulations, to a weakly nonlinear framework which applies for cross sea modelling (Cavaleri *et al.* 2012), and to test if a weakly nonlinear wave framework is sufficient to characterize all measured RWs observed in the ESBI simulations. We carried out benchmarking numerical simulations by means of the CNLS, as previously reported and parametrized for water waves (Okamura 1984; Onorato *et al.* 2006) and mentioned in the introductory Section 1. The two-wave

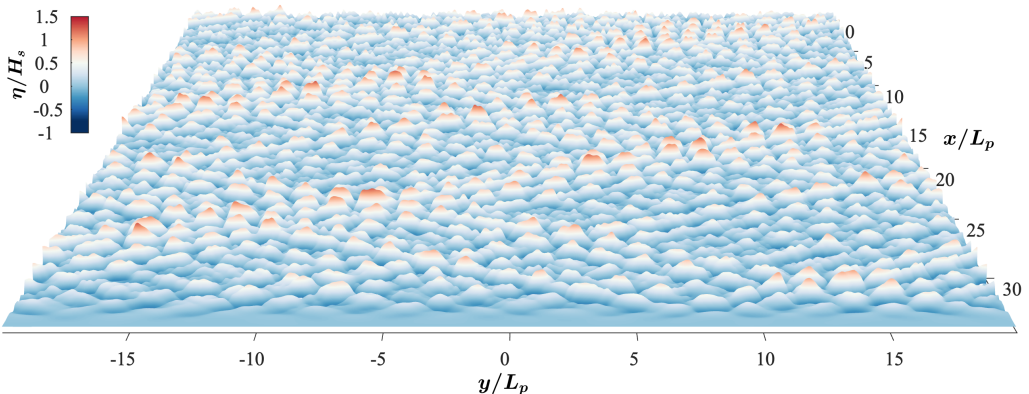


Figure 1: An exemplified snapshot example of a simulated crossing sea surface elevation of steepness  $k_p H_s = 0.28$  for a cross-interfering JONSWAP wave field with peakedness  $\gamma = 6$ .

deep-water coupled framework writes:

$$\begin{aligned} \frac{\partial u_1}{\partial t} + c_x \frac{\partial u_1}{\partial x} + c_y \frac{\partial u_1}{\partial y} - i\alpha \frac{\partial^2 u_1}{\partial x^2} - i\beta \frac{\partial^2 u_1}{\partial y^2} + i\gamma \frac{\partial^2 u_1}{\partial x \partial y} + i(\xi |u_1|^2 + 2\zeta |u_2|^2) u_1 &= 0, \\ \frac{\partial u_2}{\partial t} + c_x \frac{\partial u_2}{\partial x} - c_y \frac{\partial u_2}{\partial y} - i\alpha \frac{\partial^2 u_2}{\partial x^2} - i\beta \frac{\partial^2 u_2}{\partial y^2} - i\gamma \frac{\partial^2 u_2}{\partial x \partial y} + i(\xi |u_2|^2 + 2\zeta |u_1|^2) u_2 &= 0, \end{aligned} \quad (2.9)$$

where the coefficients write are defined as:

$$\begin{aligned} c_x &= \frac{\omega}{2\kappa^2} k, \quad c_y = \frac{\omega}{2\kappa^2} l, \quad \alpha = \frac{\omega}{8\kappa^4} (2l^2 - k^2), \quad \beta = \frac{\omega}{8\kappa^4} (2k^2 - l^2), \\ \xi &= \frac{1}{2} \omega \kappa^2, \quad \zeta = \frac{\omega}{2\kappa} \frac{k^5 - k^3 l^2 - 3kl^4 - 2k^4 \kappa + 2k^2 l^2 \kappa + 2l^4 \kappa}{(k - 2\kappa)\kappa}, \\ k &= \kappa \cos \theta, \quad l = \kappa \sin \theta. \end{aligned} \quad (2.10)$$

Here,  $u_1(x, y, t)$  and  $u_2(x, y, t)$  are two crossing complex wave envelopes with wavenumbers of  $k_1 = (k, l)$  and  $k_2 = (k, -l)$ , respectively,  $\theta$  is the crossing angle, the angular frequency  $\omega$  and the modulus of their wavenumbers  $\kappa$  obey the deep-water dispersion relation  $\kappa = \omega^2/g$ , where  $g$  is the gravitational acceleration. Note that when  $\theta = 0$ ,  $u_2$  is inactive, and therefore, Equation (2.9) is uncoupled and naturally reduces to the classical NLS (Zakharov 1968). The first-order approximation of a two-wave-field crossing elevation  $\eta(x, y, t)$  is given by:

$$\eta(x, y, t) = \frac{1}{2} \left( u_1(x, y, t) e^{i(kx+ly-\omega t)} + u_2(x, y, t) e^{i(kx-ly+\omega t)} + c.c. \right), \quad (2.11)$$

where *c.c.* denotes the complex conjugation. To ensure highest numerical accuracy, fourth-order Runge-Kutta and pseudospectral methods (Yang 2010) are adopted to advance Equation 2.9 in time. The two equations are coupled in a staggered manner, as already adopted by He *et al.* (2022) to validate laboratory observations. The corresponding numerical results will be reported and compared to the fully nonlinear ESBI results in Subsection 3.3.



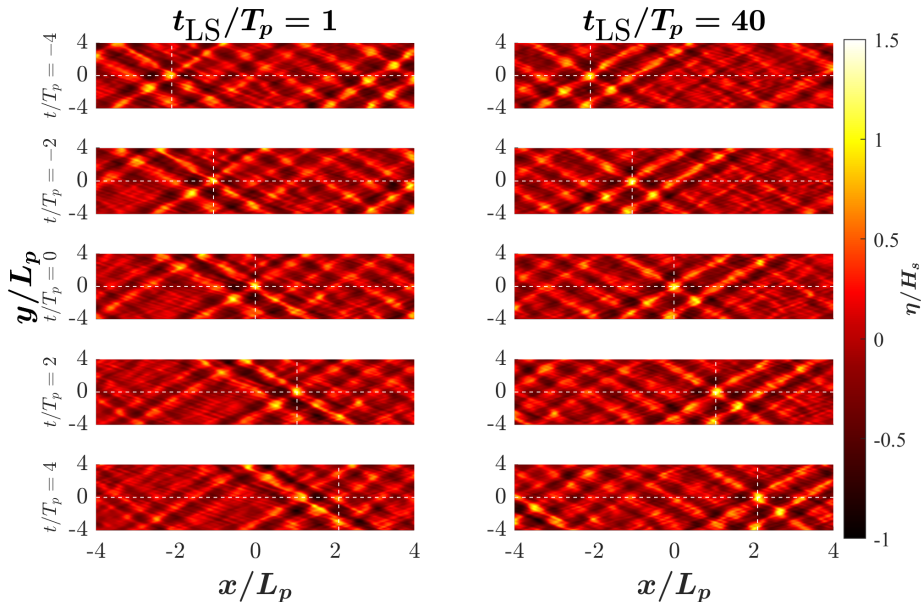


Figure 2: Comparison of two exemplary cross-RW events with different lifespans  $t_{LS}$ , evolving from the top to bottom in each column. The mean-direction wave field evolution is plotted every two peak wave periods  $T_p$ . When  $t/T_p = 0$ , the current RWs reach their peak. The left five subplots show a short-lifespan RW event with  $t_{LS} = 1T_p$  only. The subplots on the right show a long-lifespan RW event with  $t_{LS} = 40T_p$ . The orthogonal white dashed lines indicate the location of the compared RW events relative to the reference center point. Both cases are extracted from the numerical JONSWAP sea state simulations for  $k_p H_s = 0.28$  as already described in Figure 1.

### 3. Lifespan Analysis of Emerged Rogue Waves and Categorization

We begin by reasonably assuming that crossing RWs develop along the mean wave direction (Onorato *et al.* 2006), and trivially define that two RWs are considered part of one "event" if their adjacent distance does not exceed two wavelengths in the mean wave direction and 0.8 wavelengths in the perpendicular direction. In addition to that, the latter events must occur within a time interval not exceeding five periods. Thus, the *lifespan* of an independent event  $t_{LS}$  can be defined as:

$$t_{LS} = t_{RW,end} - t_{RW,ini}, \quad (3.1)$$

where  $t_{RW,ini}$  and  $t_{RW,end}$  are the occurrence time of the first and last identified RW in an identified extreme localization event. In particular, we refer to the events with  $t_{LS}/T_p = 1$  as those short-lived ones with a lifespan less than one peak wave period.

From Figure 2, two representative RWs with different  $t_{LS}$  are compared, suggesting that RWs appearing at different time scale lengths along the mean wave direction can be observed within the same crossing wave field. To simplify the further analysis, we will treat such cases as *independent events* while the first class of such events being conjectured as a result of wave interference, due to the very short focusing time.

#### 3.1. Spatio-Temporal Evolution of Long-Lived Directional Coherent RW Structures

To further examine whether the observed long-lived localized wave structures experience both growth and decay, and thus indeed obey the definition of a RW, we depict

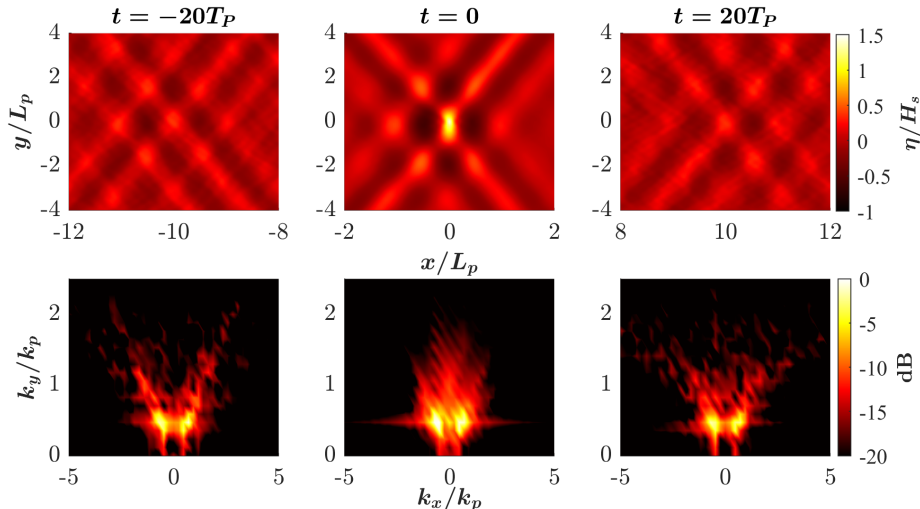


Figure 3: Spatio-temporal evolution of the mean 3D RW events with long-lifespan ( $t_{LS} > 35T_p$ ) and JONSWAP peakedness factor  $\gamma = 3$  at three different stages of extreme focusing evolution:  $20T_p$  before the peak, at the peak ( $t = 0$ ), and  $20T_p$  after the peak, which correspond to the left, middle, and right plots, respectively. Upper plots: The mean elevation field. Lower plots: Corresponding mean wave energy spectra.

in Figure 3 the mean spatio-temporal evolution of all long-lifespan RW elevation fields followed by the corresponding mean directional spectra.

In the current figure, we can observe a strong wave amplitude focusing followed by a decay in both  $x$  and  $y$ -directions, as well as the broadening and narrowing of the directional spectrum. From the current observation, we show that a clearly detectable *long-lived breathing-type* process can occur in directional seas, as suggested by our fully nonlinear framework simulations. Thus, these observed directional and particular RW structures can be a result of nonlinear interactions, which yield to a *full* localization in time and directional space. To the best of our knowledge such pulsating wave phenomenon with such longevity features was so far not reported and not discussed by means of fully nonlinear numerical simulations.

To further characterize and distinguish these RW events in such irregular cross sea states, it is important to extract key statistical characteristics, which will be analyzed and discussed as next.

### 3.2. Statistical Analysis of RW Events in Crossing Seas

In the following, we extract all independent events from the numerical data and calculate their corresponding probability density function (PDF) with a categorization with respect to both,  $t_{LS}$  and maximum wave crest height  $\eta_{\max}$  of the extreme events. As shown in Figure 4, the PDFs of all independent events are generated with respect to the maximum amplification factor and the normalized lifespan for all six JONSWAP- $\gamma$  cases with the identical  $H_s$  values as mentioned earlier. The results indicate that most independent events have a short lifespan, suggesting that wave superposition principle is a dominant focusing mechanism for our modelled cross sea states. That being said, around one in  $10^3$  to  $10^5$  events exhibits significantly longer lifespan, depending on the JONSWAP peakedness parameter  $\gamma$  value considered, with a trend of increasing amplification factor by gradually narrowing the initial energy spectrum. Such an observations indicate



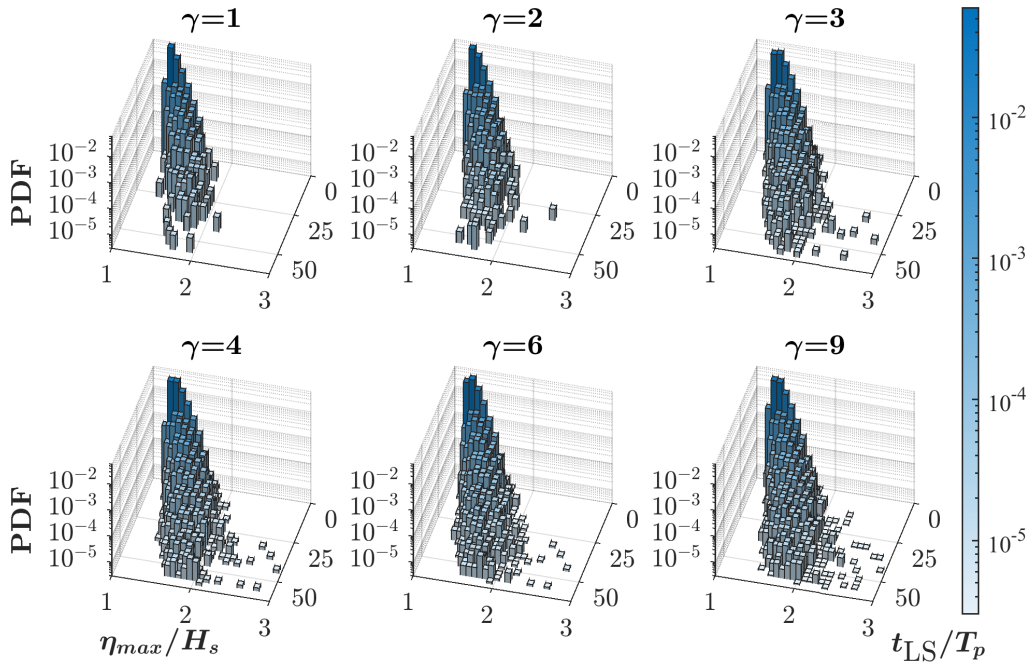


Figure 4: Statistical PDF results of the correlation between the amplification factors, defined as  $\eta_{\max}/H_s$ , their lifespans  $t_{\text{LS}}$  as RWs along the mean wave directions, and the probability density function while considering different JONSWAP spectral peakedness parameter  $\gamma$  values.

the existence of a nonlinear focusing mechanism responsible for such wave amplifications, despite having a low probability. However, the fact that such rogue waves are recurrent, i.e., experience recurrent focusing, these can indeed still pose a significant threat in the ocean.

To interpret these nonlinear RW events, as we will call these from now on, we analyze the events according to their lifespans and the spectral directionality measured by the "Full Area Half Maximum" (FAHM), see Figure 5. Since the distributions of the RWs are highly non-uniform along the  $t_{\text{LS}}/T_p$  axis, a good linear fit and reasonable clustering can be achieved upon averaging all original RW elevation data along the  $t_{\text{LS}}$  axis within every certain interval, in our case chosen to be  $t_{\text{LS}}/T_p = 0.6$ .

Surprisingly, those nonlinear RW events with longer lifespans show greater FAHM levels, suggesting the occurrence of a long-term broadening of the directional wave spectrum. Here, we highlight the work by [Toffoli \*et al.\* \(2010\)](#), which numerically observed the development of a similar bimodal pattern in the spectra. Meanwhile, the analysis by [Osborne & Ponce de León \(2017\)](#) shows that an initial and single JONSWAP spectrum can also become directionally-unstable along the modulation channel. However, these strongly relevant studies were not directly related to the formation of full-spatial localized and directional RW structures. For further ease of the analysis, the RW events under each  $\gamma$  case considered in Figure 5 are categorized into three K-means clusters ([Lloyd 1982](#); [Arthur \*et al.\* 2007](#); [Cremonini \*et al.\* 2021](#)), by using different colors, each representing a group of independent RW events with different FAHM and lifespan ranges. Note that the clustering is mainly used to group the many RW data observed from the simulations,

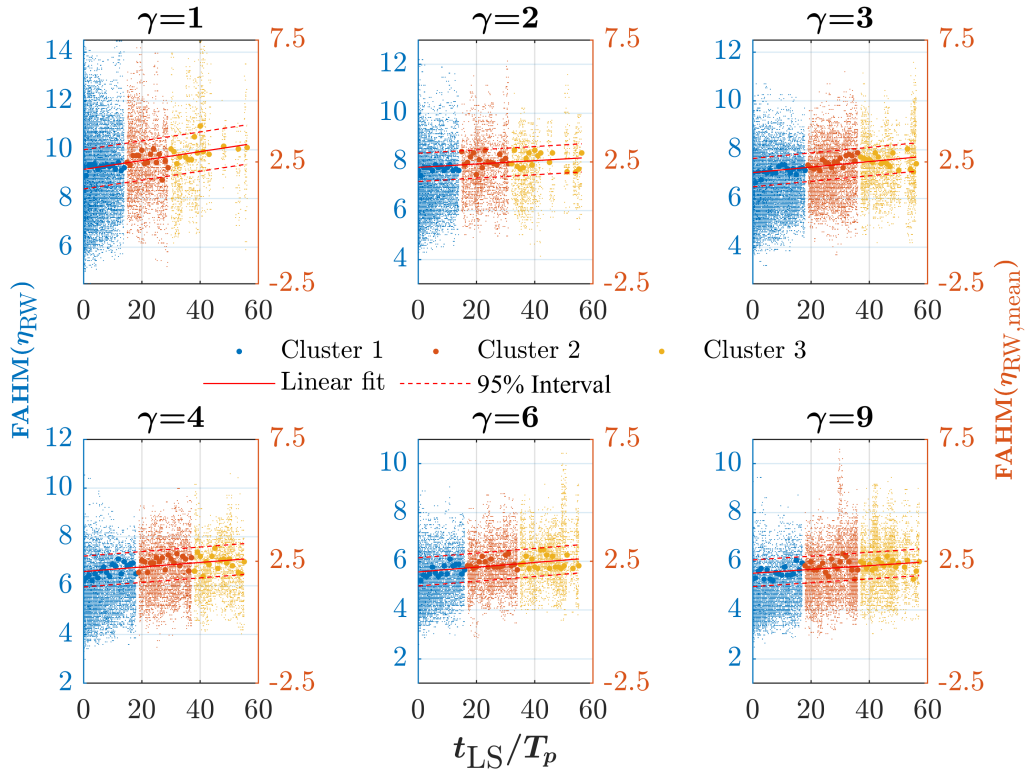


Figure 5: The correlation between the RWs' lifespans  $t_{LS}/T_p$  and their directional FAHM factor. The left  $y$ -axis represents the FAHM values of all RWs visualized by minor dots, and the right  $y$ -axis shows the FAHM values of the mean RW elevation fields (instead of the mean FAHM value) depicted by thicker dots. Here, an averaging interval of  $t_{LS} = 0.6$  is used. Considering the mean FAHM, the data are categorized into three K-means clusters in different colors. The linear fit and 95% confidence interval are also given for each case.

and is achieved by adopting the K-means++ algorithm as developed by [Arthur \*et al.\* \(2007\)](#), which is more effective than the standard K-means algorithm ([Lloyd 1982](#)).

Upon averaging the RW events within each cluster and while tracking the directional wave elevation field evolution, we can notice in [Figure 6](#) deviations from the New Wave theory ([Taylor & Williams 2004](#)), with lifetime  $t_{LS}/T_p = 1$  (bottom row), increases with the increase of  $t_{LS}$  or the cluster number, especially, for Cluster 3, in which the elevation fields are nearly independent of the initial JONSWAP-peakedness  $\gamma$  values and form four dark wave trough holes around the center peak.

Whether such a coherent structure implies a possible deterministic description of so-called higher-dimensional nonlinear RWs, like it is the case for NLS breathers for unidirectional wave states, needs future attention.

The shape of these extreme waves is similar to the ones already reported in ([Liu \*et al.\* 2022](#)). Differently to the latter work, we focus our analysis on the longevity of the rogue wave events while considering one collision angle only and varying the JONSWAP peakedness parameter.

Next, we show the corresponding spectra of all cases discussed and shown in [Figure 7](#), confirming once again the significant broadening of the directional spectrum from short-

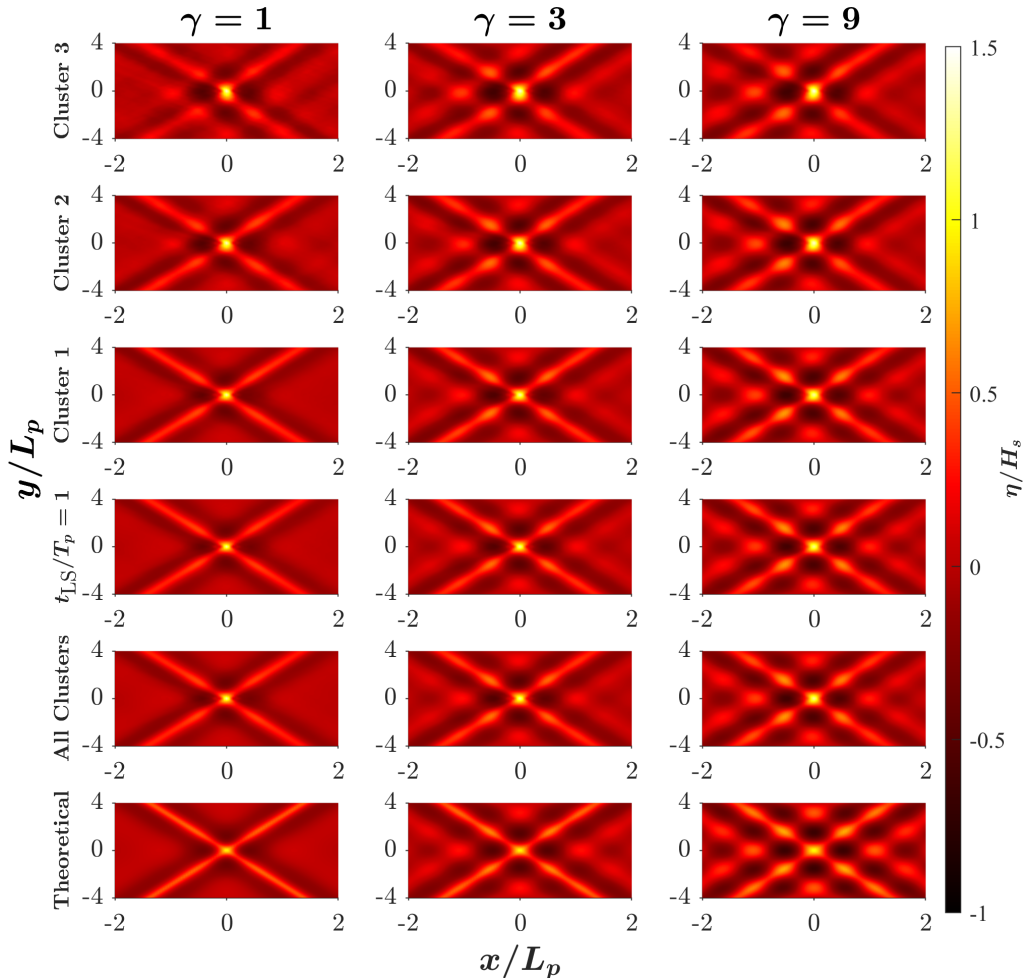


Figure 6: 3D averaged RW wave local elevation field, truncated according to the three K-means clusters from Figure 5 (top three rows) according to Figure 5, and compared with the averaged RW elevation field calculated from all  $t_{\text{LS}} = 1T_p$  cases corresponding to one-RW events (third-bottom row), with all RW events as reference (second-bottom row), and the corresponding second-order New Wave Theory spectrum (bottom row). Only three representative JONSWAP peakedness parameter factors  $\gamma=1, 3,$  and  $9$  are considered in the current figure.

to long-lived  $t_{\text{LS}}$  RW events. Note that with longer  $t_{\text{LS}}$ , the directional spectrum gradually differs from the wave interference case, which is rather characterized by remaining narrowband in the two wave directions after the extreme wave focusing. Despite, from both Figures 6 and 7, one can notice that averaging all RW events can easily lead to the neglect of Clusters 2 and 3, which are the most affected by nonlinearity and directional spreading, develop of a dual bimodal structure in the spectrum. It is therefore recommended to consider and adopt an appropriate aggregated approach to analyze the real-world RW data (Häfner *et al.* 2021).

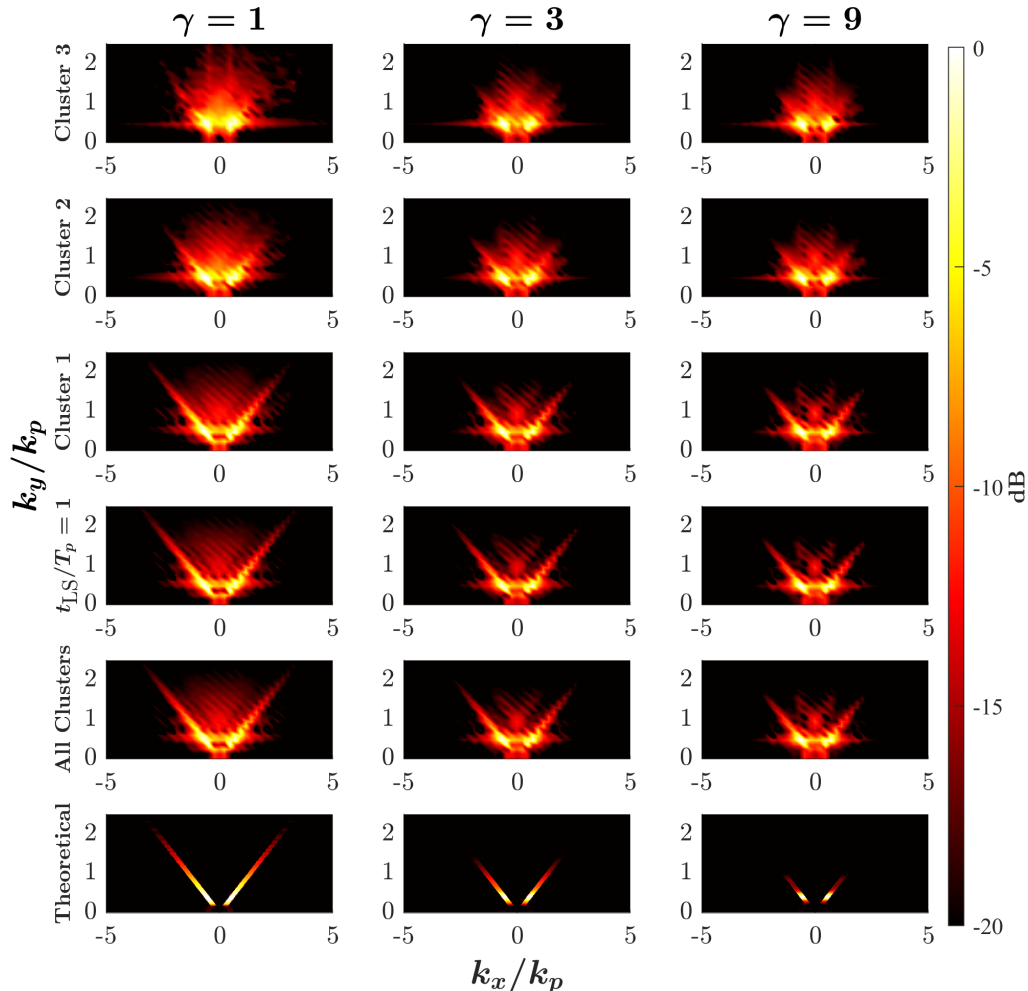


Figure 7: 3D averaged RW local spectra corresponding to Figure 6.

### 3.3. Comparison with the CNLS Framework

In order to further understand the role of nonlinearity and particularly the degree and order in the manifestation of these coherent directional large-amplitude waves in a crossing sea setup, we compare the obtained fully nonlinear results with the CNLS framework simulations.

Classified into three K-means clusters, the directional and localized RW elevation results in Figure 8 show a trend similar to those in Figure 6 for a low significant wave height  $H_s = 0.015$  m of the JONSWAP wave field generated in each direction with  $\gamma = 9$ . Such wave height scales have been chosen to motivate future laboratory experiments. Differences in averaged wave envelope shapes are noticeable in Figure 8, particularly for the long-lived extreme waves, which are clumped in Cluster 2 and 3. The directional spectra in Figure 9 further confirm a typical and expected spectral broadening in both fully and weakly nonlinear frameworks. In fact, the CNLS predicts a broader initial spectrum and reduced dual bimodality trend, compared to the fully nonlinear ESBI simulations.

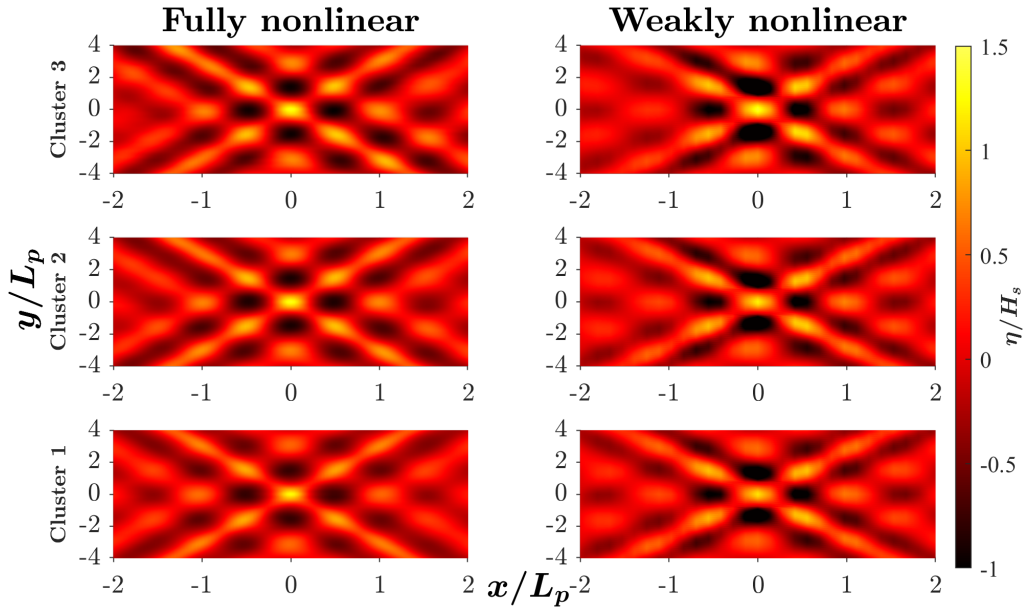


Figure 8: Comparison of directional and averaged RW wave local elevation field simulated by means of the fully nonlinear (ESBI) framework (left panels) and the corresponding CNLS simulations (right panels). The generate JONSWAP wave field has a significant wave height of  $H_s = 0.015$  m with  $\gamma = 9$ .

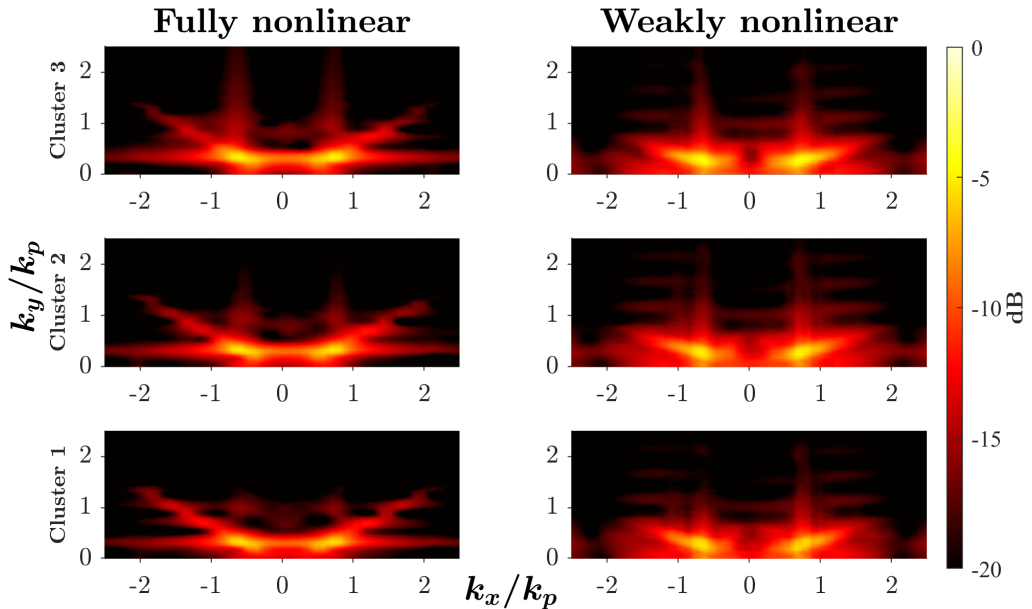


Figure 9: Comparison of the corresponding averaged RW wave local spectra corresponding to Figure 8.

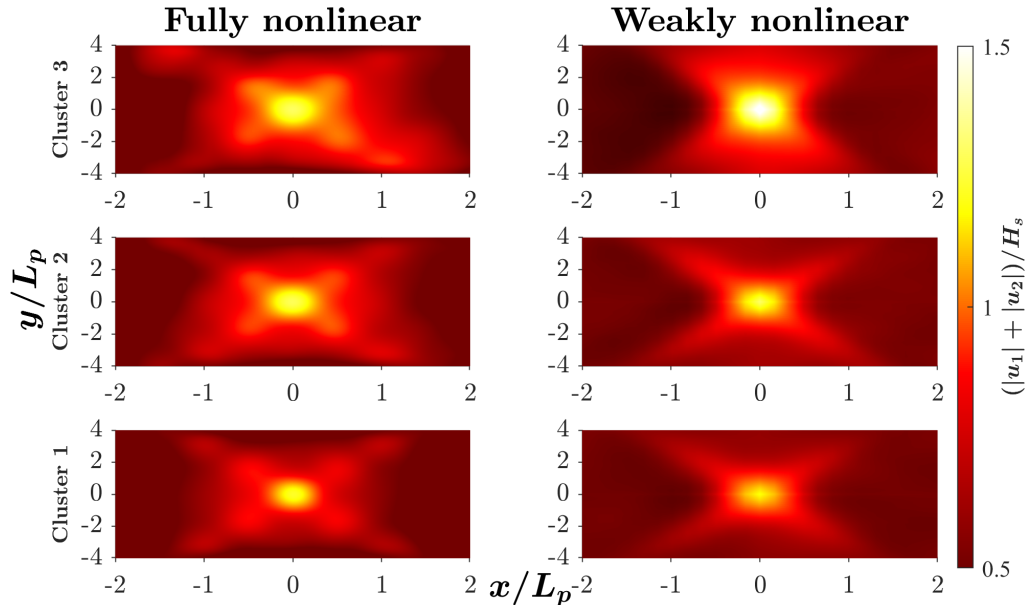


Figure 10: Comparison of the magnified and directional averaged localized maximal envelope peak shapes corresponding to Figure 8.

Intriguingly, one can clearly observe the differences in the extreme wave envelope peak, as magnified in Figure 10. While the Cluster 1 wave envelopes at the bottom of the figure, which appear to be the result of wave overlap, have a quasi-similar pattern, the long-lived extreme events in Cluster 2 and 3 show a completely different and distinct shape when simulated by the fully and weakly nonlinear framework. Such directional localized wave patterns cannot be analytically modelled thus far. A complete and quantitative characterization of these coherent extreme waves requires comprehensive future numerical and experimental explorations.

#### 4. Discussion and Conclusion

This paper investigates key physical and statistical properties of RW events in crossing JONSWAP-type sea states using a fully nonlinear ESBI framework (Wang *et al.* 2021a) and a lifespan-based analysis approach (Chabchoub *et al.* 2012; Kokorina & Slunyaev 2019). We focus on a specific crossing angle of 40 degrees and analyze RWs under different JONSWAP spectrum bandwidths (Toffoli *et al.* 2011; Cavaleri *et al.* 2012; Bitner-Gregersen & Toffoli 2014).

Our numerical ESBI results reveal RW events developing along the mean wave direction with lifespans ranging from  $1T_p$  while satisfying the RW threshold criterion, up to  $40T_p$  and beyond. For these long-lasting nonlinear RW events, we observe a clear focusing and decay process of the mean directional wave elevation field, along with a perfect recurrence of the mean directional wave spectrum. This suggests that wave superposition and the classical (unidirectional) MI (Benjamin & Feir 1967; Mori *et al.* 2011) are insufficient for the prediction of all extreme wave events in such realistic directional seas.

On the other hand, we further analyze the statistical characteristics of such occurring crossing RW events by varying the JONSWAP peakedness factor  $\gamma$  and find that the probability of long-lifespan events increases by increasing  $\gamma$ , highlighting the potential



role of quasi-four wave resonant interactions in one of the two colliding wave beams, which might be not substantially influenced by the other wave field component. Moreover, previous studies point to the significance of spreading effects (Toffoli *et al.* 2010) as well as directional weakly nonlinear effects (Osborne & Ponce de León 2017) in the RW generation. The emergence of the localized severe and typical spectral broadening followed by a dual bimodality further supports the role of nonlinear wave interactions in the formation of RWs in cross seas.

Furthermore, classifying RW events into three clusters based on their corresponding lifespans reveals a gradual deviation of the mean wave elevation and energy spectra from the New Wave theory (superposition principle) with increasing longevity of the extreme wave events.

In order to explore the role of weakly nonlinear effects in the lifetime of RWs, we compare the fully nonlinear ESBI numerical results with the weakly nonlinear CNLS simulations. Both frameworks exhibit very good qualitative agreement, with consistent changes in wave elevation patterns and directional spectral broadening, particularly observed for increasing extreme event lifespans. Interestingly, Cluster 3, which regroups the long lifespan extreme wave envelopes, reveals unique discrepancies in the RW coherence when modeled by ESBI and the CNLS. This is likely due to the limitations of the CNLS approach (Liu *et al.* 2022) and of the Hilbert transformation for such wave systems. While predicting such extreme localizations analytically is to date not possible, the spatio-temporal localized and directional RW solutions (Qiu *et al.* 2016; Guo *et al.* 2020) offer promising avenues for future investigation.

In conclusion, this work unveils a characteristic type of directional nonlinear and coherent RW structure in crossing seas, highlighting the role of nonlinear wave interaction in the formation of extreme events in colliding two-wave systems. The obtained RWs are characterized by short and long lifespans along the mean wave direction while the corresponding directional spectrum broadening is followed by a distinct dual bimodal pattern. We also confirm the sufficient role of CNLS to qualitatively simulate such long-lived freak waves. Further theoretical and experimental studies are necessary to fully comprehend and predict these nonlinear waves, beyond the limitations of the wave setup and the CNLS framework as adopted in this work.

## 5. Acknowledgement

Y.H. acknowledges the support from the Distinguished Postdoctoral Fellowship Scheme of the Hong Kong Polytechnic University (PolyU). Y.H. and J.W. show gratitude to the sponsorship provided by the University Grants Committee, Hong Kong (P0039692), PolyU, Hong Kong (A0048708), Research Institute for Sustainable Urban Development at PolyU, Hong Kong (P0042840), Department of Science and Technology of Guangdong Province, China (22202206050000278). A.C. acknowledges support from Kyoto University's Hakubi Center for Advanced Research.

## REFERENCES

- AKHMEDIEV, NAIL, ELEONSKII, VM & KULAGIN, NE 1985 Generation of periodic trains of picosecond pulses in an optical fiber: exact solutions. *Sov. Phys. JETP* **62** (5), 894–899.
- ARTHUR, DAVID, VASSILVITSKII, SERGEI & OTHERS 2007 k-means++: The advantages of careful seeding. In *Soda*, , vol. 7, pp. 1027–1035.
- BENJAMIN, T BROOKE & FEIR, JAMES E 1967 The disintegration of wave trains on deep water part 1. theory. *Journal of Fluid Mechanics* **27** (3), 417–430.
- BIRKHOFF, SIMON, BRÉE, CARSTEN, VESELIĆ, IVAN, DEMIRCAN, AYHAN & STEINMEYER,

- GÜNTER 2016 Ocean rogue waves and their phase space dynamics in the limit of a linear interference model. *Scientific reports* **6** (1), 35207.
- BITNER-GREGERSEN, ELZBIETA M & TOFFOLI, ALESSANDRO 2014 Occurrence of rogue sea states and consequences for marine structures. *Ocean Dynamics* **64**, 1457–1468.
- BONNEFOY, FÉLICIEN, HAUDIN, FLORENCE, MICHEL, GUILLAUME, SEMIN, BENOÎT, HUMBERT, THOMAS, AUMAÎTRE, SÉBASTIEN, BERHANU, MICHAEL & FALCON, ERIC 2016 Observation of resonant interactions among surface gravity waves. *Journal of Fluid Mechanics* **805**.
- CANUTO, CLAUDIO, HUSSAINI, M YOUSUFF, QUARTERONI, ALFIO & ZANG, THOMAS A 1987 Spectral methods in fluid dynamics springer-verlag. *New York* .
- CAVALERI, L, BERTOTTI, L, TORRISI, L, BITNER-GREGERSEN, E, SERIO, MARINA & ONORATO, MIGUEL 2012 Rogue waves in crossing seas: The louis majesty accident. *Journal of Geophysical Research: Oceans* **117** (C11).
- CHABCHOUB, AMIN, AKHMEDIEV, NAIL & HOFFMANN, NORBERT 2012 Experimental study of spatiotemporally localized surface gravity water waves. *Physical Review E* **86** (1), 016311.
- CHABCHOUB, AMIN, HOFFMANN, NORBERT & AKHMEDIEV, NAIL 2011 Rogue wave observation in a water wave tank. *Physical Review Letters* **106** (20), 204502.
- CHABCHOUB, AMIN, MOZUMI, KENTO, HOFFMANN, NORBERT, BABANIN, ALEXANDER V, TOFFOLI, ALESSANDRO, STEER, JAMES N, VAN DEN BREMER, TON S, AKHMEDIEV, NAIL, ONORATO, MIGUEL & WASEDA, TAKUJI 2019 Directional soliton and breather beams. *Proceedings of the National Academy of Sciences* **116** (20), 9759–9763.
- CLAMOND, D., FRUCTUS, D. & GRUE, J. 2007 A note on time integrators in water-wave simulations. *Journal of Engineering Mathematics* **58**, 149–156.
- CREMONINI, GIULIA, DE LEO, FRANCESCO, STOCCHINO, ALESSANDRO & BESIO, GIOVANNI 2021 On the selection of time-varying scenarios of wind and ocean waves: Methodologies and applications in the north tyrrhenian sea. *Ocean Modelling* **163**, 101819.
- DAVEY, A & STEWARTSON, KEITH 1974 On three-dimensional packets of surface waves. *Proceedings of the Royal Society of London. A. Mathematical and Physical Sciences* **338** (1613), 101–110.
- DUCROZET, GUILLAUME, BONNEFOY, FÉLICIEN, MORI, NOBUHITO, FINK, MATHIAS & CHABCHOUB, AMIN 2020 Experimental reconstruction of extreme sea waves by time reversal principle. *Journal of Fluid Mechanics* **884**, A20.
- DUDLEY, JOHN M, GENTY, GOËRY, MUSSOT, ARNAUD, CHABCHOUB, AMIN & DIAS, FRÉDÉRIC 2019 Rogue waves and analogies in optics and oceanography. *Nature Reviews Physics* **1** (11), 675–689.
- FEDELE, FRANCESCO, BRENNAN, JOSEPH, PONCE DE LEÓN, SONIA, DUDLEY, JOHN & DIAS, FRÉDÉRIC 2016 Real world ocean rogue waves explained without the modulational instability. *Scientific reports* **6** (1), 27715.
- FRUCTUS, D., CLAMOND, D., GRUE, J. & KRISTIENSEN, Ø. 2005a An efficient model for three-dimensional surface wave simulations: Part i: Free space problems. *Journal of computational physics* **205** (2), 665–685.
- FRUCTUS, D, KHARIF, CHRISTIAN, FRANCIUS, M, KRISTIENSEN, Ø, CLAMOND, D & GRUE, J 2005b Dynamics of crescent water wave patterns. *Journal of Fluid Mechanics* **537**, 155–186.
- GRAMSTAD, ODIN, BITNER-GREGERSEN, ELZBIETA, TRULSEN, KARSTEN & NIETO BORGE, JOSÉ CARLOS 2018 Modulational instability and rogue waves in crossing sea states. *Journal of Physical Oceanography* **48** (6), 1317–1331.
- GRAMSTAD, ODIN & TRULSEN, KARSTEN 2011 Fourth-order coupled nonlinear Schrödinger equations for gravity waves on deep water. *Physics of Fluids* **23** (6), 062102.
- GRÖNLUND, ANDREAS, ELIASSON, BENGT & MARKLUND, MATTIAS 2009 Evolution of rogue waves in interacting wave systems. *EPL (Europhysics Letters)* **86** (2), 24001.
- GUO, LIJUAN, HE, JINGSONG, WANG, LIHONG, CHENG, YI, FRANTZESKAKIS, DJ, VAN DEN BREMER, TS & KEVREKIDIS, PG 2020 Two-dimensional rogue waves on zero background in a benney-roskes model. *Physical Review Research* **2** (3), 033376.
- HÄFNER, DION, GEMMRICH, JOHANNES & JOCHUM, MARKUS 2021 Real-world rogue wave probabilities. *Scientific Reports* **11** (1), 10084.
- HÄFNER, DION, GEMMRICH, JOHANNES & JOCHUM, MARKUS 2023 Machine-guided discovery of

- a real-world rogue wave model. *Proceedings of the National Academy of Sciences* **120** (48), e2306275120.
- HASSELMANN, KLAUS, BARNETT, TP, BOUWS, E, CARLSON, H, CARTWRIGHT, DE, ENKE, K, EWING, JA, GIENAPP, H, HASSELMANN, DE, KRUSEMAN, P & OTHERS 1973 Measurements of wind-wave growth and swell decay during the joint north sea wave project (jonswap). *Ergänzungsheft 8-12* .
- HE, YUCHEN, SLUNYAEV, ALEXEY, MORI, NOBUHITO & CHABCHOUB, AMIN 2022 Experimental evidence of nonlinear focusing in standing water waves. *Physical Review Letters* **129** (14), 144502.
- JANSSEN, PETER AEM 2003 Nonlinear four-wave interactions and freak waves. *Journal of Physical Oceanography* **33** (4), 863–884.
- KHARIF, CHRISTIAN, PELINOVSKY, EFIM & SLUNYAEV, ALEXEY 2008 *Rogue waves in the ocean*. Springer.
- KLAHN, MATHIAS, ZHAI, YANYAN & FUHRMAN, DAVID R 2024 Heavy tails and probability density functions to any nonlinear order for the surface elevation in irregular seas. *Journal of Fluid Mechanics* **985**, A35.
- KOKORINA, ANNA & SLUNYAEV, ALEXEY 2019 Lifetimes of rogue wave events in direct numerical simulations of deep-water irregular sea waves. *Fluids* **4** (2), 70.
- LIU, SHUAI, WASEDA, TAKUJI, YAO, JINYU & ZHANG, XINSHU 2022 Statistical properties of surface gravity waves and freak wave occurrence in crossing sea states. *Physical Review Fluids* **7** (7), 074805.
- LLOYD, STUART 1982 Least squares quantization in pcm. *IEEE transactions on information theory* **28** (2), 129–137.
- LONGUET-HIGGINS, MS 1974 Breaking waves in deep or shallow water. In *Proc. 10th Conf. on Naval Hydrodynamics*, , vol. 597, p. 605. MIT.
- MATHIS, AMAURY, FROEHLI, LUC, TOENGER, SHANTI, DIAS, FRÉDÉRIC, GENTY, GOËRY & DUDLEY, JOHN M 2015 Caustics and rogue waves in an optical sea. *Scientific reports* **5** (1), 12822.
- MCALLISTER, MARK L, DRAYCOTT, SAM, ADCOCK, TAA, TAYLOR, PH & VAN DEN BREMER, TS 2019 Laboratory recreation of the draupner wave and the role of breaking in crossing seas. *Journal of Fluid Mechanics* **860**, 767–786.
- MORI, NOBUHITO, ONORATO, MIGUEL & JANSSEN, PETER AEM 2011 On the estimation of the kurtosis in directional sea states for freak wave forecasting. *Journal of Physical Oceanography* **41** (8), 1484–1497.
- MORI, NOBUITO, WASEDA, TAKUJI & CHABCHOUB, AMIN 2023 *Science and Engineering of Freak Waves*. Elsevier.
- OKAMURA, MAKOTO 1984 Instabilities of weakly nonlinear standing gravity waves. *Journal of the Physical Society of Japan* **53** (11), 3788–3796.
- ONORATO, MIGUEL, OSBORNE, ALFRED RICHARD & SERIO, MARIANA 2006 Modulational instability in crossing sea states: A possible mechanism for the formation of freak waves. *Physical Review Letters* **96** (1), 014503.
- ONORATO, MIGUEL, PROMENT, DAVIDE & TOFFOLI, ALESSANDRO 2010 Freak waves in crossing seas. *The European Physical Journal Special Topics* **185** (1), 45–55.
- OSBORNE, ALFRED 2010 *Nonlinear Ocean Waves and the Inverse Scattering Transform*. Academic Press.
- OSBORNE, ALFRED R & PONCE DE LEÓN, SONIA 2017 Properties of rogue waves and the shape of the ocean wave power spectrum. In *International Conference on Offshore Mechanics and Arctic Engineering*, , vol. 57656, p. V03AT02A013. American Society of Mechanical Engineers.
- PEREGRINE, D HOWELL 1983 Water waves, nonlinear schrödinger equations and their solutions. *The ANZIAM Journal* **25** (1), 16–43.
- QIU, DEQIN, ZHANG, YONGSHUAI & HE, JINGSONG 2016 The rogue wave solutions of a new (2+1)-dimensional equation. *Communications in Nonlinear Science and Numerical Simulation* **30** (1-3), 307–315.
- SAFFMAN, PG & YUEN, HENRY C 1978 Stability of a plane soliton to infinitesimal two-dimensional perturbations. *The Physics of Fluids* **21** (8), 1450–1451.
- STEER, JAMES N, MCALLISTER, MARK L, BORTHWICK, ALISTAIR GL & VAN DEN BREMER,

- TON S 2019 Experimental observation of modulational instability in crossing surface gravity wavetrains. *Fluids* **4** (2), 105.
- TANG, TIANNING, XU, WENTAO, BARRATT, DYLAN, BINGHAM, HARRY B, LI, Y, TAYLOR, PH, VAN DEN BREMER, TS & ADCOCK, TAA 2021 Spatial evolution of the kurtosis of steep unidirectional random waves. *Journal of Fluid Mechanics* **908**, A3.
- TAYLOR, P. H. & WILLIAMS, B. A. 2004 Wave Statistics for Intermediate Depth Water—New Waves and Symmetry. *Journal of Offshore Mechanics and Arctic Engineering* **126** (1), 54–59, arXiv: [https://asmedigitalcollection.asme.org/offshoremechanics/article-pdf/126/1/54/5506470/54\\_1.pdf](https://asmedigitalcollection.asme.org/offshoremechanics/article-pdf/126/1/54/5506470/54_1.pdf).
- TIKAN, ALEXEY, BONNEFOY, FELICIEN, ROBERTI, GIACOMO, EL, GENNADY, TOVBIS, ALEXANDER, DUCROZET, GUILLAUME, CAZAUBIEL, ANNETTE, PRABHUDESAI, GAURAV, MICHEL, GUILLAUME, COPIE, FRANCOIS & OTHERS 2022 Prediction and manipulation of hydrodynamic rogue waves via nonlinear spectral engineering. *Physical Review Fluids* **7** (5), 054401.
- TOFFOLI, ALESSANDRO, ALBERELLO, ALBERTO, CLARKE, HANS, NELLI, FILIPPO, BENETAZZO, ALVISE, BERGAMASCO, FILIPPO, NTAMBA, BUTTEUR NTAMBA, VICHI, MARCELLO & ONORATO, MIGUEL 2024 Observations of rogue seas in the southern ocean. *Physical Review Letters* **132**, 154101.
- TOFFOLI, ALESSANDRO, BITNER-GREGERSEN, EM, OSBORNE, ALFRED RICHARD, SERIO, MARINA, MONBALIU, JAAK & ONORATO, MIGUEL 2011 Extreme waves in random crossing seas: Laboratory experiments and numerical simulations. *Geophysical Research Letters* **38** (6).
- TOFFOLI, ALESSANDRO, ONORATO, MIGUEL, BITNER-GREGERSEN, EM & MONBALIU, JAAK 2010 Development of a bimodal structure in ocean wave spectra. *Journal of Geophysical Research: Oceans* **115** (C3).
- TULIN, MARSHALL P 1996 Breaking of ocean waves and downshifting. In *Waves and nonlinear processes in hydrodynamics*, pp. 177–190. Springer.
- TULIN, MARSHALL P & WASEDA, TAKUJI 1999 Laboratory observations of wave group evolution, including breaking effects. *Journal of Fluid Mechanics* **378**, 197–232.
- WANG, JINGHUA 2023 An enhanced spectral boundary integral method for modeling highly nonlinear water waves in variable depth. *arXiv preprint arXiv:2310.19840*.
- WANG, JINGHUA & MA, QINGWEI 2015 Numerical techniques on improving computational efficiency of spectral boundary integral method. *International Journal for Numerical Methods in Engineering* **102** (10), 1638–1669.
- WANG, JINGHUA, MA, QINGWEI & YAN, SHIQIANG 2018 A fully nonlinear numerical method for modeling wave–current interactions. *Journal of Computational Physics* **369**, 173–190.
- WANG, JINGHUA, MA, QINGWEI, YAN, SHIQIANG & LIANG, BINGCHEN 2021a Modeling Crossing Random Seas by Fully Non-Linear Numerical Simulations. *Frontiers in Physics* **9**, 593394.
- WANG, JINGHUA, MA, QINGWEI, YAN, SHIQIANG & LIANG, BINGCHEN 2021b Modeling crossing random seas by fully non-linear numerical simulations. *Frontiers in Physics* **9**, 593394.
- WASEDA, TAKUJI 2020 Nonlinear processes. In *Ocean Wave Dynamics*, p. 103. World Scientific.
- WASEDA, TAKUJI, KINOSHITA, TAKESHI & TAMURA, HITOSHI 2009 Evolution of a random directional wave and freak wave occurrence. *Journal of Physical Oceanography* **39** (3), 621–639.
- WASEDA, TAKUJI, WATANABE, SHOGO, FUJIMOTO, WATARU, NOSE, TAKEHIKO, KODAIRA, TSUBASA & CHABCHOUB, AMIN 2021 Directional coherent wave group from an assimilated non-linear wavefield. *Frontiers in Physics* **9**, 622303.
- XIAO, WENTING, LIU, YUMING, WU, GUANGYU & YUE, DICK KP 2013 Rogue wave occurrence and dynamics by direct simulations of nonlinear wave-field evolution. *Journal of Fluid Mechanics* **720**, 357–392.
- YANG, JIANKE 2010 *Nonlinear waves in integrable and nonintegrable systems*. SIAM.
- ZAKHAROV, VLADIMIR E 1968 Stability of periodic waves of finite amplitude on the surface of a deep fluid. *Journal of Applied Mechanics and Technical Physics* **9** (2), 190–194.